



Identification of jamming transition: a critical appraisal

Mingze Xu^{1,2} · Zixin Zhang^{1,2} · Xin Huang^{1,2}

Received: 6 March 2020 / Accepted: 1 October 2020 / Published online: 26 November 2020
© Springer-Verlag GmbH Germany, part of Springer Nature 2020

Abstract

A variety of approaches have been proposed to determine the onset of jamming (unjamming) transition for granular medium. However, these approaches all have their own limitations. In this study, the applicability of the existing approaches in identifying the jamming (unjamming) transition instant is evaluated based on the discrete element method simulations on both frictionless and frictional specimens subjected to different loading protocols which lead to isotropic jamming, shear jamming and shear unjamming. A new approach based on Hill's criterion of failure is proposed, which defines the transition of second order work from positive to negative as the onset of jamming (unjamming) transition. The jamming (unjamming) transition instant determined from the new approach is compared with those determined from some classic approaches. It is found that the second order work-based approach not only locates the critical solid fraction in the jamming diagram consistent with other approaches, but is also able to identify the onset of jamming (unjamming) transition for loading protocols that are difficult to be assessed by the existing approaches. This more robust approach is useful for the study of jamming phenomena under a broader types of loading protocols, and can be further employed to derive the jamming diagram of real materials.

Keywords Jamming transition · Critical solid fraction · Second order work

1 Introduction

Jamming is defined as a state that a particulate system can sustain external forces without deforming irreversibly [1]. When subject to infinitesimal external perturbations, such as temperature change or shear, a particulate system may flow like liquid in the unjamming state but will behave closely to solid once the jamming (unjamming) transition state has been reached. It is non-trivial to macroscopically ascertain whether a particulate system is jammed; therefore, the jamming state is deemed to be reached when the number of mechanical equilibrium constraints reaches the number of degrees of freedom, i.e., the system becomes isostatic [1]. Necessary conditions characterizing a jammed state include

non-zero mean stress, shear stress and ability to sustain small incremental stress. The transition from the unjammed state to the jammed state is generally referred to as jamming (unjamming) transition. It is a characteristic state distinguishing a solid phase from a liquid phase.

Jamming (unjamming) transition has been extensively investigated by previous researchers due to its importance in the powder related industry and understanding of the physics underlying behaviors of granular medium. In order to describe this transition and link to its influential factors, a jamming diagram was proposed by Liu and Nagel [2], in which they defined the jamming and unjamming zone based on three quantities, i.e., temperature, solid fraction and shear stress. The original jamming diagram was improved by successive researchers. For example, Ciamarra et al. [3] introduced friction as an additional coordinate axis in the jamming diagram to consider the frictional properties of different materials. Bi et al. [1] further identified a shear jamming zone and a fragile zone between the original jamming and unjamming zones.

A premise of a rational analysis on the jamming phenomena and establishment of the jamming diagram is the correct identification of jamming (unjamming) transition point. For systems which are athermal and experience no shear stress,

This article is part of the Topical Collection: Flow regimes and phase transitions in granular matter: multiscale modeling from micromechanics to continuum.

✉ Xin Huang
xhuang@tongji.edu.cn

¹ Department of Geotechnical Engineering, Tongji University, Shanghai 200092, China

² State Key Laboratory of Geotechnical and Underground Engineering, Tongji University, Shanghai 200092, China

a number of well-defined approaches have been developed to determine the critical solid fraction (ϕ_j). In such cases, a granular system is in a jammed state when its solid fraction is above ϕ_j , while it is in an unjammed state when its solid fraction is below ϕ_j . Göncü et al. [4] discussed the ϕ_j values obtained from different approaches considering the influences of the number of particles, polydispersity and loading rate. Nonetheless, when the systems are subjected to more realistic complex loading protocols with different forms of shear stress variation, the identification of jamming (unjammed) transition is nontrivial, particularly for frictional systems. Since frictionless materials are rarely encountered in the real world and the loading conditions that a real material may experience are more complex than isotropic loading, it is necessary to establish a more robust approach that can identify the jamming transition phenomena of real materials subject to realistic loading scenarios. This is the major motivation of the current study.

In this study, a brief summary of the existing approaches for identifying the jamming (unjammed) transition is firstly provided. A series of DEM simulations on both frictionless and frictional systems are conducted considering different loading protocols including isotropic compression, constant-volume triaxial compression, and constant-volume cyclic triaxial compression. A new approach of identifying jamming-unjamming transition is proposed based on the second order work principle. The applicability of different approaches in identifying the jamming (unjammed) transition under various loading scenarios is evaluated, based on which the robustness and reliability of the new approach are demonstrated. The limitations of the newly proposed approach are also discussed.

2 A brief review of existing approaches for identifying jamming (unjammed) transition

In order to determine the onset of jamming (unjammed) transition, different approaches have been developed. The most prevailing ones are summarized below:

2.1 Coordination number-based approach

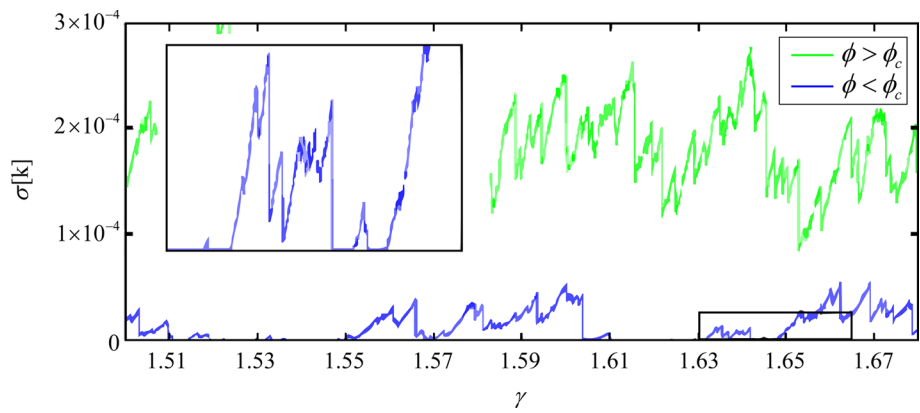
This is the most widely used criterion. Theoretically, for a frictionless particulate system, it is mechanically stable (isostatic or hyperstatic) only when the coordination number C^r , which is defined as $C^r = M/N$, reaches 6 for 3D system and 4 for 2D system, where N is the total number of particles and M is twice the total number of contacts. But for frictional systems, it is difficult to find a precise threshold value for the coordination number at the isostatic state. Researchers can only give a minimum value for mechanical stability [5, 6] or

use the so-called isostatic coordination number (Z_{iso}) [7, 8]. Theoretically, the isostatic coordination number lies between $d+1$ and $2d$ depending on the frictional coefficient [5], in which d denotes the dimension of the system which is 2 for a 2D system and 3 for a 3D system. Different definitions of C^r have been proposed in order to exclude the influence of rattlers. For example, Imole et al. [9] proposed using the corrected coordination number C^* which is defined as $C^* = M_4/N_4$, in which M_4 is the total number of contacts owned by the N_4 mechanically stable particles with at least 4 contacts. Thornton [10] defined a mechanical coordination number Z_m to be $Z_m = 2(N_c - N_p^1)/(N_p - N_p^1 - N_p^0)$, where N_c is the total number of contacts, N_p is the total number of particles, N_p^1 and N_p^0 are the number of particles with one contact and zero contact, respectively. For the frictionless particles, this coordination number criterion (either modified or not) has a solid theoretical foundation and has been used extensively [5, 9, 11–14].

2.2 Yield stress-based approach

Apart from the coordination number criterion, inspired by the definition of jamming, the onset of yield stress is used as a criterion by several researchers [15–18]. The yield stress is the applied stress that must be exceeded in order to make a structured fluid flow [19]. Similar to shear modulus, the shear yield stress is a material property that distinguishes solids from liquids [16]. Heussinger and Barrat [20] gave an example of identifying yield stress during shearing under the constant volume condition, as can be seen in Fig. 1, in which the green line corresponds to the sample with a solid fraction ϕ larger than the critical value (ϕ_c) and the blue line corresponds to the sample with ϕ slightly smaller than ϕ_c . In their simulations, if the volume fraction is larger than ϕ_c , the yield stress can be observed (the green line) but when the volume fraction is slightly smaller than ϕ_c , the system shows a coexistence of the yield-stress and zero-stress states (the blue line). If the volume fraction is small enough, the system will flow at zero stress state. For clarity, when no shear stress is imposed on the sample, the critical solid fraction is marked as ϕ_j which is consistent with the jamming diagram proposed by Bi et al. [1] and when shear stress exists, the critical solid fraction is denoted as ϕ_c . Similarly, Otsuki and Hayakawa [21] treated the onset of shear stress in the extremely low shear rate ($\dot{\gamma} \rightarrow 0$) as the onset of jamming (unjammed) transition and they also observed the existence of yield stress for densely packed systems. This approach was also used by Ciamarra et al. [3]. However, this approach only applies for shear jamming scenarios under the constant volume condition because it is difficult to directly observe the onset of apparent yield stress due to the fluctuation of stress in other kinds of shearing simulations or experiments.

Fig. 1 Illustration of yield stress (Heussinger and Barrat [20])



Therefore, this method is more appropriate to be used to justify whether the system is in a jammed state rather than to identify the onset of jamming (unjamming) transition.

2.3 Pressure-based approach

Similar to the yield stress-based approach, the pressure-based approach can be seen as a supplement to the yield stress-based approach. During the decompression of a particulate system, the static pressure drops to zero when it transforms from the jammed state to the unjammed state because of the loss of the particle contacts. Here, the static pressure p is the 1/3 trace of the averaged micromechanical stress, which is defined as $\bar{\sigma}_{ij} = \frac{1}{V} \sum_{c \in V} f_i^c l_j^c$, where V is the total volume of the particulate system, f_i^c is the force of contact c and l_j^c is the corresponding branch vector. In order to reduce the influence of stress fluctuation, the relationship $\frac{P}{C^* \phi} = P_{ref} \log\left(\frac{\phi}{\phi_c}\right)$ was used by Göncü et al. [4], where $P = pr_0/k_n$ is the normalized pressure, r_0 is the averaged radius, k_n is the normal contact stiffness and P_{ref} is a fitting parameter.

2.4 Rattler-based approach

In 3D simulations, the rattler is normally defined as a particle with fewer than 4 contacts [4, 9]. The number of rattlers surges up abruptly when the system transforms from the jammed state to the unjammed state, and vice versa. This method has been used to identify the critical solid fraction in the isotropic compression simulation [4, 22]. It is more common to use the non-rattler fraction (f_{NR}) to determine the onset of jamming (unjamming) transition. The non-rattler fraction f_{NR} is defined as $f_{NR} = N_4/N$, where N_4 is the number of particles with at least 4 contacts and N is the number of particles in the particulate system. Bi et al. [1] observed in their 2D photo-elastic experiments that when a system reached the jammed state, $f_{NR} = 0.83 \pm 0.02$ under pure shear condition. This was confirmed later by Kumar et al.

[11] in their 3D pure shear DEM simulations. However, this approach is not universally applicable, i.e., the jump of the number of rattlers is more obvious during decompression than under compression. Furthermore, the threshold value of f_{NR} has no theoretical explanations, and whether it is applicable for loading conditions other than pure shear is unknown.

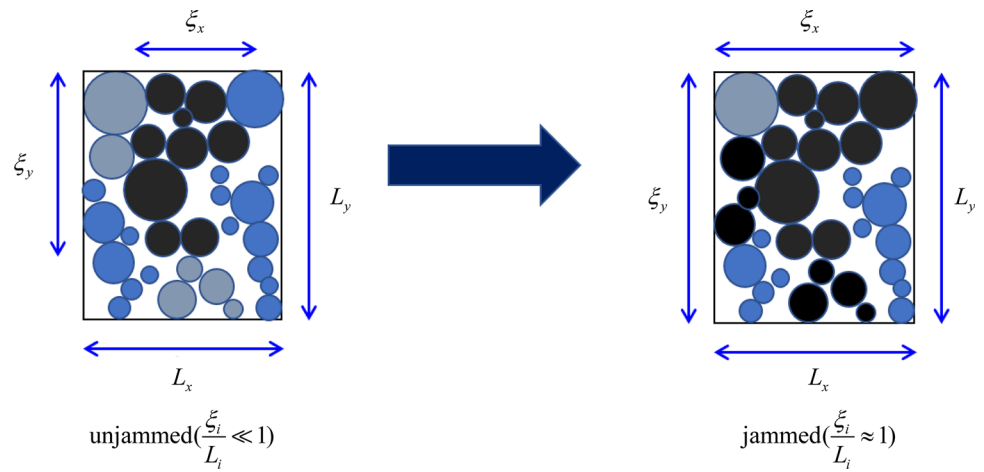
2.5 Energy-based approach

The values of the jamming density ϕ_j can also be obtained based on the ratio between the kinetic energy (E_{kin}) and potential energy (E_{pot}) of the system, which is expressed by $e = E_{kin}/E_{pot}$ [23]. The jammed state is defined as the point where the compression branch of the $e-\phi$ curve crosses its decompression branch [4]. However, the accuracy of this method strongly depends on the spacing of the data points around the jamming (unjamming) transition point. Furthermore, there is also no theoretical explanation for this intersection.

2.6 Percolation analysis-based approach

Bi et al. [1] proposed using percolation analysis on the force transmission network to determine the shear jamming-unjamming (unjamming) transition in their photo-elastic experiments. As can be seen in Fig. 2, the jammed state is reached when the granular system comes to a percolated state in all dimensions, i.e., $\xi_x/L_x = \xi_y/L_y = \xi_z/L_z = 1$ (3D), where ξ_i is the length of the largest force transmission network and L_i is the sample dimension in the i th direction. Here, the largest force transmission network is comprised of strong contacts which bear contact forces larger than a characteristic value that is several times of the average contact force, i.e., $f \geq kf_{avg}$, where k is a magnification factor. However, the determination of k is rather empirical and may be affected by many factors including the problem dimension (2D or 3D), disparity of particle size and loading conditions, etc. Bi et al. [1] used $k=1$ for 2D disks and other researchers used $k=2.2$ for 3D spheres [11, 24, 25]. The other limitation

Fig. 2 2D Sketch map of percolation analysis



of this approach is that for most of real materials, it is difficult to obtain the contact information required for percolation analysis. Therefore, the applicability of percolation analysis-based approach is restricted to idealized simulations or photo-elastic experiments.

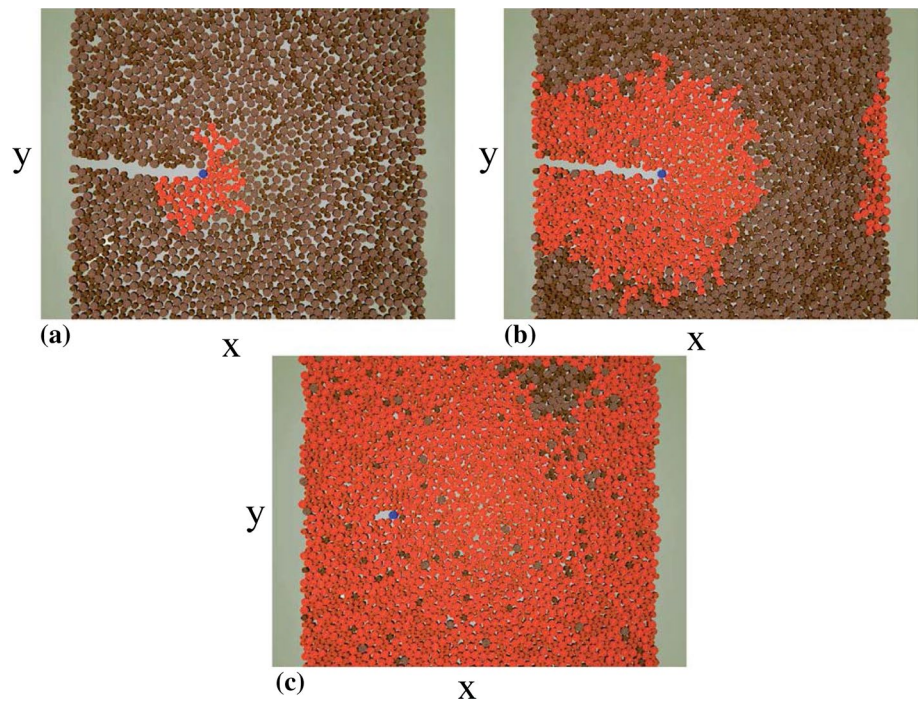
2.7 Perturbation length-based approach

Some researchers used perturbation length to determine whether or not the sample reaches the isostatic state [26–29]. In this method, a probe particle driven by a constant force is forced to travel from one boundary side of the system to the opposite side, during which the number of disturbed particles is recorded (Fig. 3). The perturbation length is defined

as the ratio between the number of disturbed particles and the total number of particles. When the perturbation length is large enough, the system is in a jammed state; otherwise it is in an unjammed state. This method seems to be practical but the threshold value of the perturbation length is totally empirical, which makes it difficult to determine the jamming (unjamming) transition point precisely. Furthermore, when this method is applied, a state that is close to the jamming (unjamming) transition point needs to be estimated beforehand so that loading can be stopped at this point to conduct the perturbation probe, which unavoidably will disturb the original structure of the system.

Overall, different approaches have been proposed to identify the jamming (unjamming) transition point of granular

Fig. 3 Sketch map of perturbation length-based method (Reichhardt et al. [29])



medium. As summarized in Table 1, each approach has its own merits but also limitations. In general, the coordination number-based approach is difficult to apply for frictional systems, while determinations of the threshold value are empirical for other approaches. Furthermore, most of the existing approaches require micro-scale information regarding the interaction between particles, which is difficult to be obtained for real materials.

3 A new method of determining jamming (unjamming) transition

Since the current approaches determining the jamming (unjamming) transition all have some limitations, a more robust approach which can be applicable for both frictionless and frictional systems subject to various types of loading conditions is needed. In geomechanics, the Hill’s criterion is widely used to examine the stability of soils. Based on this criterion, a macroscopic expression of second order work was used to check the stability of soil [30, 31],

$$W_2 = (d\varepsilon_v dp + d\varepsilon_q dq) * V \tag{1}$$

in which ε_v is the volumetric strain, p is the mean stress, ε_q and q are the deviatoric strain and the deviatoric stress, V is the volume of the particulate system, respectively. Subject to a specific loading condition, when W_2 is strictly larger than 0, the soil is in a stable state; otherwise, instabilities occur [34]. The relationship between the second order work and entropy source has been proved to be equivalent, and Hill’s condition is consistent with the second law of thermodynamics [31]. The second order work could also be expressed

using microscopic variables accounting for the microstructure of the particulate system [32]:

$$W_2^\mu = \sum_{p,q} \delta f_i^{fc} \delta l_i^c + \sum_{p \in V} \delta f_i^p \delta x_i^p. \tag{2}$$

The first term in Eq. 2 is related to the contact force network, in which l_i^c is the branch vector and f_i^c is the contact force of the i th contact between the contacting particles p and q , while the second term is related to the incremental unbalanced force and incremental change in position of particle, where x_i^p is the position and f_i^p is the resultant force of particle p along the i th direction. The vanishing second-order work marks the bifurcation of soil behavior from quasi-static regime to dynamic regime, which is characterized by the coincidence between the onset of instability and the outburst of kinetic energy [33]. This was later nicely proved analytically by Nicot et al. [34, 35]. The second order work (either macroscopic or microscopic) criterion, which has a solid theoretical basis, has been shown to effectively distinguish between the stable and unstable states [30–32, 36]. Unstable state in soil mechanics is usually defined as a state when infinitesimal perturbations will lead to finite changes of the system’s state [37]. It is a broader concept encompassing unjamming as the former does not imply a zero-stress state while the latter does. Therefore, although it has been pointed out by Nova [38] and Buscarnera et al. [39] that the Hill’s condition is insufficient to determine the state of the soil since the material stability is not only an intrinsic characteristic but also relates to the control parameters in soil mechanics, it is still reasonable to use it as a criterion to identify the onset of jamming because the stable state (jamming state) used in this paper is different from that in the classical soil mechanics and the jamming transition is

Table 1 Overview of current criteria of determining jamming (unjamming) transition

| Approaches | Merits | Limitations |
|-------------------------------------|---|--|
| Coordination number-based approach | 1. A precise threshold value for frictionless particle systems 2. A solid theoretical foundation | No precise threshold value for frictional particle systems |
| Yield stress-based approach | Inspired by the jamming definition and has a solid theoretical foundation | 1. Only suitable for shearing condition 2. Hard to observe in the simulations or experiments |
| Stress-based approach | A precise value can be provided | Can only be used under isotropic decompression |
| Rattler-based approach | – | The number of rattler method is more suitable for isotropic decompression condition Threshold f_{NR} has only been validated under pure shear condition |
| Energy-based approach | – | The accuracy strongly depends on the spacing of the data points |
| Percolation analysis-based approach | Easy to implement in both the simulations and photo-elastic experiments | Selection of k value is empirical |
| Perturbation length-based approach | Easy to implement in both the simulations and photo-elastic experiments | Threshold value is empirical and the probe trial will disturb the sample |

more similar to the bifurcation of soil behavior. Besides, as pointed out by Hadda et al. [36] and Nicot et al. [34], the second order work criterion can effectively detect the failure induced by the incremental loading in one particular direction and can be further linked with the use of directional analysis. The vanishing of the second-order work is adopted herein as a new approach to identify the jamming (unjamming) transition state of granular medium under different loading conditions. In comparison to previous approaches, the second-order work approach has the following merits:

- the criterion of identifying jamming (unjamming) transition, i.e., W_2 or $W_2'' = 0$, is independent of problem dimension, friction property, disparity of particle size and loading conditions
- the quantities involved in calculation can be easily obtained both experimentally and numerically.

Apart from the merits, the limitations of the second order work criterion also need to be acknowledged. Firstly, micro-scale formulation of the second order work is only reliable in the quasi-static condition. Secondly, there are also some scenarios at which an instability (peak) state appears before the unjamming state, e.g., for very loose specimen with the solid fraction slightly above the critical value, when it is subjected to constant volume shearing we will see an instability state (peak) occurs before the flow liquefaction state (unjamming) [40]. The specimen is in a jammed state when evolving from the instability state to the flow liquefaction state. Despite of these limitations, we will show below that the Hill's criterion is a more robust approach which is applicable for jamming-unjamming transition identification under a wide range of realistic loading conditions in comparison with existing approaches.

Since the main objective of this research is to prove that the second order work criterion is more robust in determining the onset of jamming (unjamming) transition for a particulate system, it should be proved that the second-order work approach can effectively identify the jamming (unjamming) transition point under different loading conditions for both frictionless and frictional systems. It has to be firstly proved for scenarios in which the jamming (unjamming) transition point can be derived theoretically, i.e., the frictionless systems; then it will be extended to more general frictional systems. The results of second-order work approach should also be compared with the results derived by other methods whose applicability has been well-recognized under certain conditions. In particular, the percolation analysis is used as a major counterpart since it seems to be applicable for all types of loading conditions. The shearing condition is not examined for the frictionless system because it cannot maintain a stable state as all the related quantities oscillate severely during shearing. Note that as pointed out by Nicot et al. [34,

35], the macro and micro expressions of second-order work may not be exactly identical, especially when approaching the instability state. This may be attributed to inertia effects which is a possible missing link between micro and macro second-order work in granular media. Therefore, the micro formulation (Eq. 2) is selected in the present paper.

4 Model setup and simulation procedures

The simulations are conducted using a modified version of the open-source LAMMPS code (Plimpton, 1995). A uniform strain rate field (affine deformation) is imposed on the particles in a periodic cubic cell. The polydisperse particle size distribution follows that of Toyoura sand (Fig. 4) which has a size ratio between the largest and the smallest particles of 3.55. The particle density was 2650 kg/m^3 without consideration of gravity. A linear elastic model was adopted with a normal contact stiffness (k_n) of $1 \times 10^8 \text{ N/m}$ and a tangential contact stiffness (k_s) of $6.67 \times 10^7 \text{ N/m}$. 20,186 non-contacting spherical particles were generated within a cubic periodic cell at an initial solid fraction (ϕ_0) of 0.5. The damping coefficient is set to be 0.1 in order to reduce the dynamic influence. The simulations were divided into five groups with different frictional and loading conditions:

Group I: A frictionless sample was firstly compressed until the solid fraction ϕ reaches 0.63, which was close to the jamming point. It was then relaxed until a nearly non-contacting condition was reached, after which the sample was compressed again at the selected compression rates until the jamming state was reached. Then, the decompression process was conducted at the same velocity. This loading process is similar to that used in Kumar et al. [11].

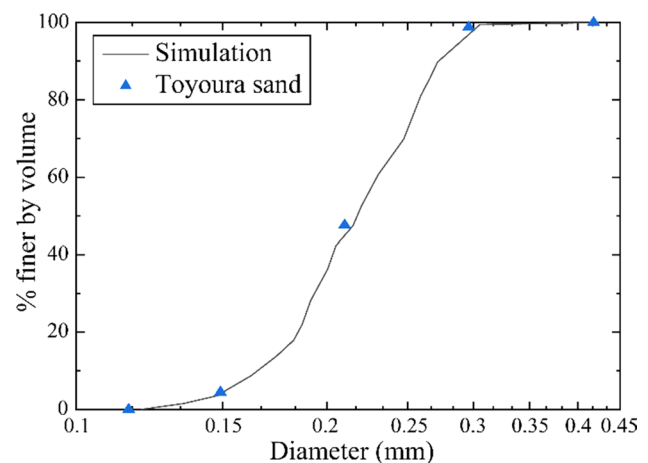


Fig. 4 Comparing the particle size distributions of the DEM samples and real Toyoura sand

Table 2 Simulation details

| ID | Solid fraction, ϕ_0 | Initial confining pressure, $\sigma_{3,0}$ (kPa) | μ during loading | Loading type | q_{cyc} (kPa) |
|-------|--------------------------|--|----------------------|--------------|-----------------|
| GI | 0.5 | 0 | 0 | Monotonic | – |
| GII | | | 0.25 | | |
| GIII | 0.6164 | 0 | 0.25 | Monotonic | – |
| GIV-1 | 0.6327 | 100 | 0.25 | Cyclic | 10 |
| GIV-2 | 0.6327 | 100 | 0.25 | | 5 |
| GV | 0.5913 | 500 | 0.5 | Monotonic | – |

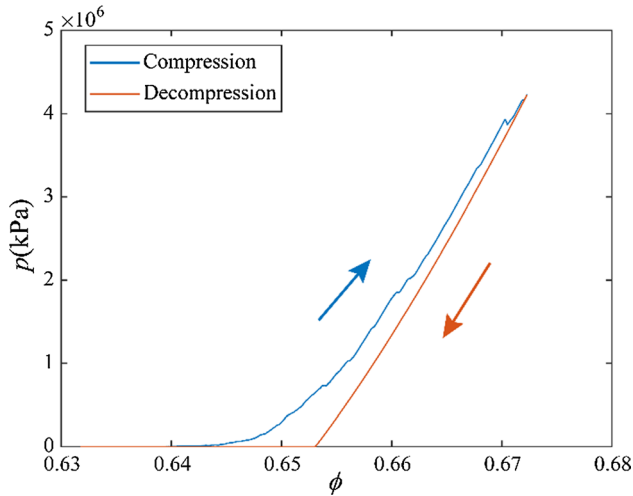


Fig. 5 p - ϕ curve during isotropic compression and decompression for a frictionless system

Group II: A sample composed of particles with an interparticle friction of 0.25 was directly compressed to reach a jammed state and then decompressed to an unjammed

state. The isotropic compression velocity was 0.025 m/s for Groups I and II which can ensure the loading process was consistently quasi-static.

Group III: The third group conducted constant-volume triaxial compression on a frictional system. An unjamming sample with a solid fraction ϕ of 0.6164 was selected from the second group, which was subjected to pure shear under a constant-volume condition. The axial compression strain rate is 0.85 s^{-1} .

Group IV: The fourth group performed constant-volume cyclic triaxial loading on a frictional system. Isotropic jammed samples at different p levels were prepared. The samples were then subjected to constant-volume sinusoidal cyclic triaxial shearing following the stress path given below:

$$q = q_{cyc} \sin(\omega t) \tag{3}$$

where q_{cyc} denotes the cyclic deviatoric stress amplitude, ω is the angular loading frequency equaling $10\pi \text{ rad/s}$, and t is the running time. This loading protocol is widely used by the geotechnical community to assess the liquefaction potential of sands [7, 41, 42].

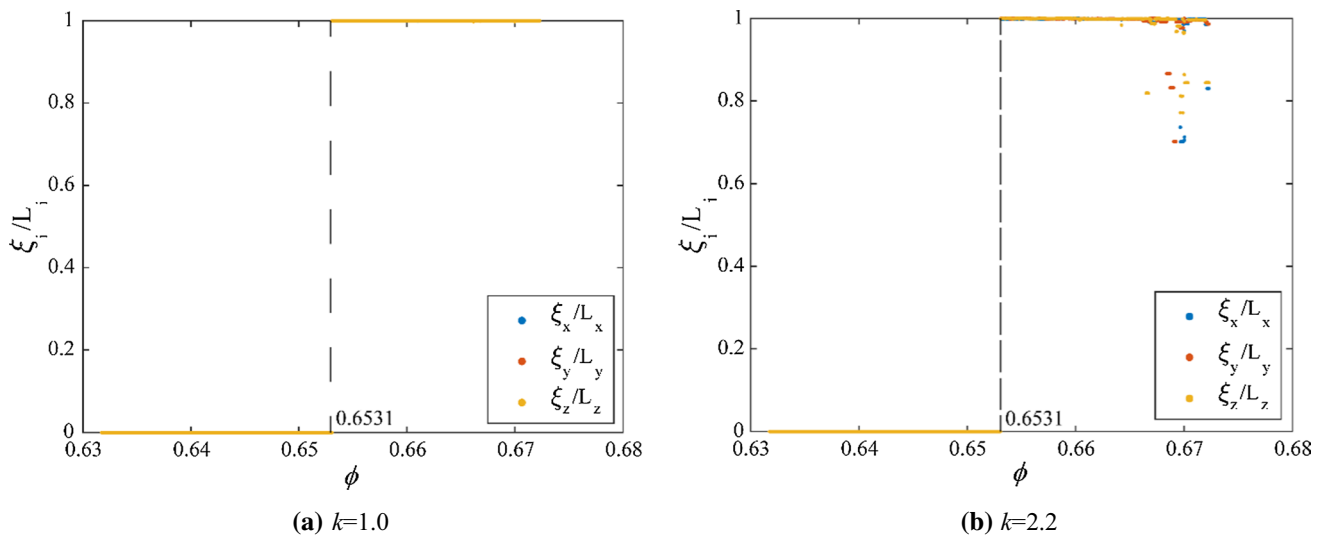


Fig. 6 Percolation analysis with different k values during isotropic decompression for a frictionless system

Group V: The last group conducted constant-volume triaxial compression on an initially jammed frictional sample. A specimen with an initial confining pressure = 500 kPa was generated, which was then subjected to triaxial shearing under constant volume condition. The axial compressive strain rate is 0.5 s^{-1} . More simulation details are given in Table 2.

5 Results and discussion

5.1 Isotropic decompression on a frictionless system

For the Group I simulations, the relationship between p and ϕ during isotropic compression and decompression is shown

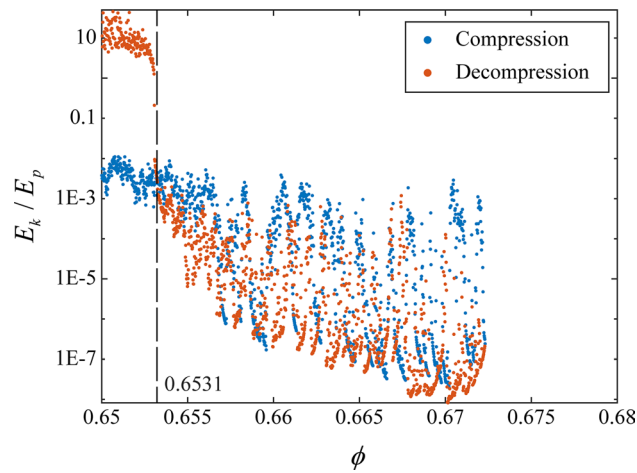


Fig. 7 Variation of the ratio of kinetic energy to potential energy during isotropic compression and decompression of a frictionless system

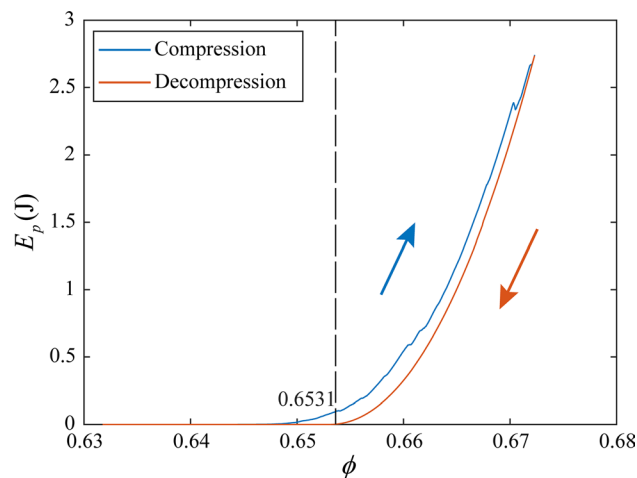


Fig. 8 Evolution of potential energy during isotropic compression and decompression for a frictionless system

in Fig. 5. During the compression process, p remains approximately zero until ϕ approaches 0.64, after which it surges up in a power-law manner. In the decompression process, p decreases as ϕ drops and approaches zero when ϕ is below 0.6531. Percolation analysis is performed to investigate the growth and interconnection of the major force transmission network. Only decompression results are listed here since the dynamic influence can be effectively reduced during decompression [22] and only in this occasion can percolation analysis be reliable. As shown in Fig. 6a, when $k = 1.0$ [1], an abrupt transition from the unpercolated to percolated states is apparent (marked by dashed line), while if $k = 2.2$ [11] is used to define the strong contacts, some oscillations in the percolation indices, ξ_i/L_i , can be observed at the initial

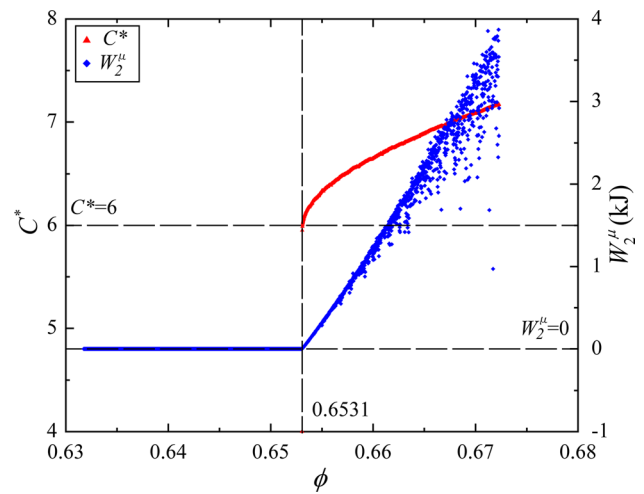


Fig. 9 Comparison between isotatic states determined using the $C^* = 6$ criterion and the $W_2^\mu = 0$ criterion for a frictionless system

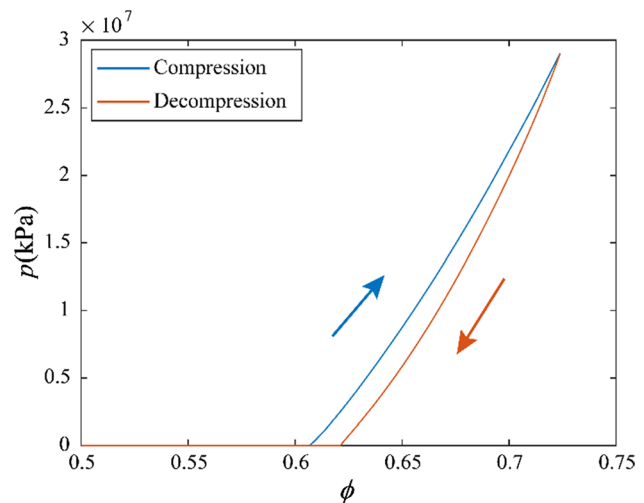


Fig. 10 p - ϕ curve during isotropic compression and decompression of a frictional system

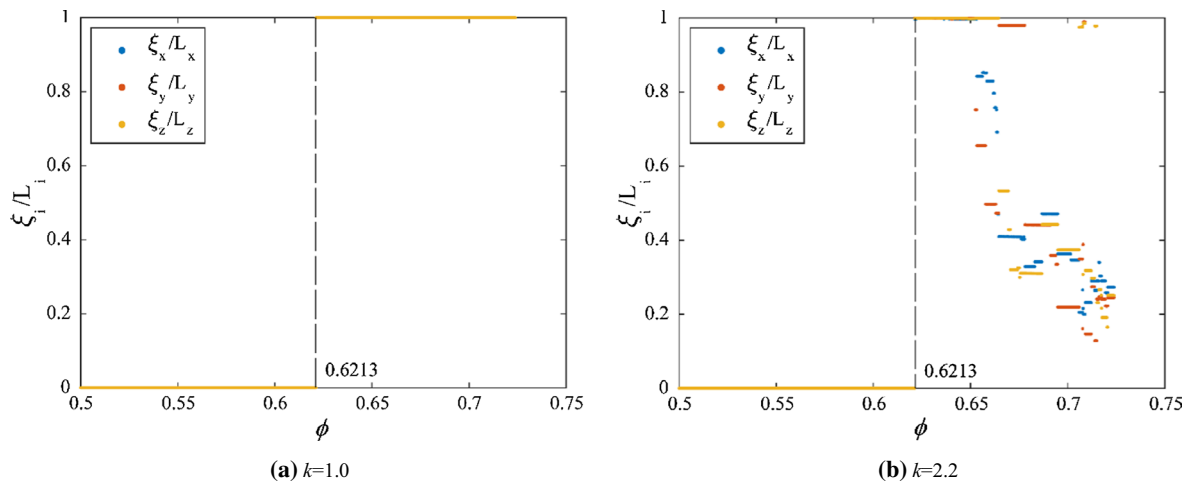


Fig. 11 Percolation analysis with different k during isotropic decompression for a frictional system

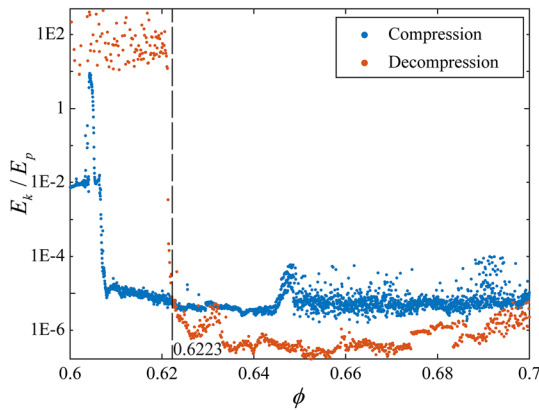


Fig. 12 The ratio of kinetic and potential energy during isotropic compression and decompression for a frictional system

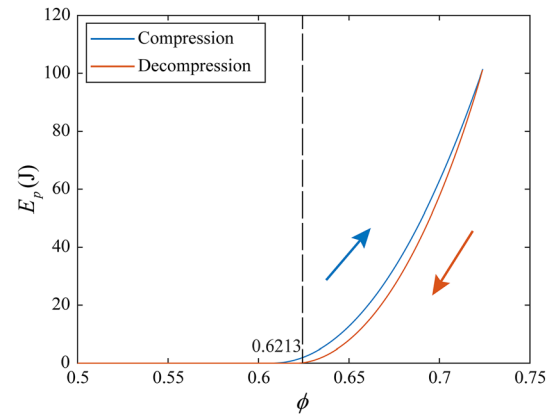


Fig. 13 Potential energy during isotropic compression and decompression for a frictional system

stage of decompression. The oscillations soon disappear in the successive decompression process. The same transition point identified by $k = 1.0$ and 2.2 indicates that the k values of 1.0 and 2.2 adopted by previous researchers [1, 11, 24, 25] are applicable to distinguish the unpercolated/unjammed and percolated/jammed states for frictionless systems during decompression coincidentally. Figure 7 shows the evolution of the ratio of kinetic energy to potential energy, E_k/E_p , during the compression and decompression process. The first crossing point of the compression and decompression curves which marks the transition point in [4] is observed at $\phi = 0.6531$ in this simulation. Besides, the drop of the potential energy to approximately zero (Fig. 8) does occur at the same solid fraction in this simulation, which also marks the jamming (unjammed) transition according to [4, 43]. For

the frictionless system, $C^* = 6$ is a well-recognized criterion marking the isostatic state. It is used here as a contrastive criterion. As can be seen in Fig. 9, the coordination number decreases gradually during decompression, and it drops sharply below 6 when ϕ decreases to 0.6531. The second order work W_2^H also decreases during the decompression process and the $W_2^H = 0$ condition is realized almost at the same time as C^* drops to below 6.

5.2 Isotropic decompression on a frictional system

The relationship between p and ϕ for the frictional system under isotropic compression and decompression (Group II) is illustrated in Fig. 10. The overall trend is similar to the frictionless system as shown in Fig. 5 except that transition occurs at a different solid fraction, and there are less

noticeable stress oscillations during the compression process. As shown in Fig. 11, percolation analysis based on the $k=1.0$ force network clearly shows a critical instant separating the unpercolated and percolated states. The percolation indices remain steadily around 1 until ϕ is reduced to 0.6213, at which all the three percolation indices drop to zero. However, if k is set to be 2.2, the percolation indices of the identified force network fluctuate severely during decompression. If the fluctuation is ignored, there is also an abrupt drop in the percolation indices and the identified $\phi_J=0.6213$ is consistent with that obtained for the $k=1.0$ force network. If the energy-based approach is applied for this frictional system, the first intersection point between the compression and decompression data can be derived at $\phi=0.6223$ (see Fig. 12). As Fig. 13 shows, a transition point can also be identified at $\phi=0.6213$ when the potential energy drops to zero which is close to the state derived in Fig. 12. Due to the additional constraints provided at the frictional contacting surface, the $C^*=6$ criterion does no more correspond to the isostatic state for a frictional system. Huang et al. [7] proposed the following formula to calculate the isostatic coordination number, Z_{iso} , for 3D frictional systems:

$$Z_{iso} = 12 / (3 - f_s), \tag{4}$$

in which f_s is the fraction of sliding contacts. Z_{iso} is reduced to 4 for rigid contacts with $f_s=0$, while it equals to 6 when $f_s=1$, which is analogous to the frictionless condition. The proposition of Z_{iso} extends the applicability of coordination number-based approach to frictional systems, in which the jamming (unjamming) transition point is defined as the intersection of the Z_{iso} curve and Z_m curve. Obviously, the accuracy of this method depends on the spacing of the data points around the jamming point. As shown in Fig. 14, Z_m decreases gradually during decompression, while Z_{iso} increases gradually during decompression due to the increase of f_s . Z_m is consistently larger than Z_{iso} until the solid fraction ϕ decreases to 0.6213, i.e., jamming (unjamming) transition occurs. Z_{iso} swaps between 4 and 6 after jamming (unjamming) transition and Z_m drops to 0. The isostatic state determined by the $W_2^H=0$ criterion exactly matches the one determined from the intersection of Z_m and Z_{iso} .

5.3 Monotonic shearing on a frictional system (shear jamming)

Figure 15 shows the stress–strain relationships during constant-volume shearing of an initially unjammed frictional system with $\phi=0.6164$ (*Group III*). The mean effective stress p and the deviatoric stress q remain almost zero at the initial state and then start to increase simultaneously when the axial strain ϵ_a exceeds 5.783%, showing a typical shear jamming scenario. As can be seen from

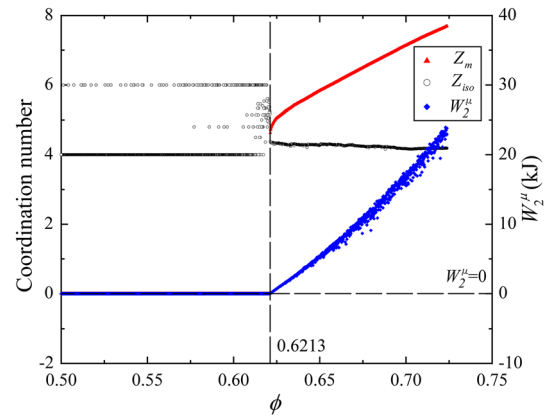


Fig. 14 Comparison between isostatic states derived based on the isostatic coordination number-based approach and the second order work-based approach for frictional particles

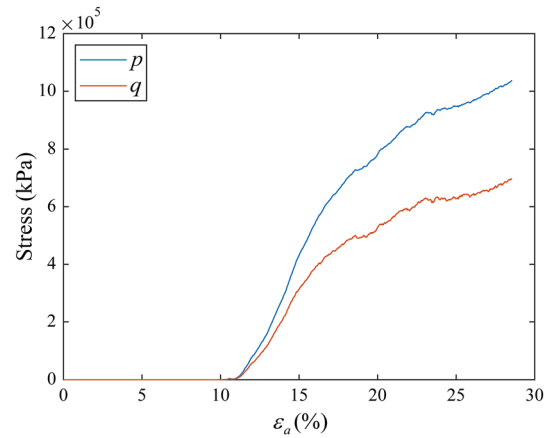


Fig. 15 Stress strain curves during constant volume monotonic shearing for a frictional system

Fig. 16, similar to *Group II* simulations shown in Fig. 11, a clear jamming transition point can be derived based on the $k=1.0$ force network when ϵ_a exceeds 7.932%. For the $k=2.2$ force network, the z -direction (compressive direction) percolation index (yellow dots) becomes consistently close to 1 when ϵ_a exceeds 10.54%, while the percolation indices in the other two directions oscillate. Therefore, it is difficult to evaluate whether or not the specimen is in a jammed state. As can be seen in Fig. 17, the initially zero Z_m starts to increase when ϵ_a reaches 5.911%, while despite some scatters, Z_{iso} remains consistently around 4. Z_m is smaller than Z_{iso} until ϵ_a exceeds 8.393%, i.e., jamming transition occurs. The transition point derived from the isostatic coordination number-based approach does not coincide with that determined from the stress–strain curve.

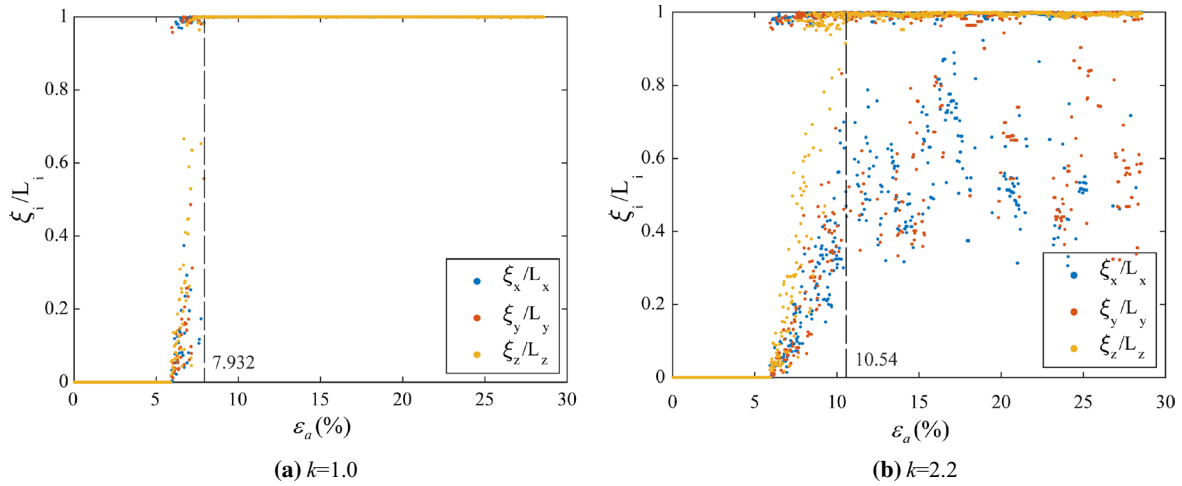


Fig. 16 Percolation analysis with different k values during constant volume monotonic shearing of a frictional system

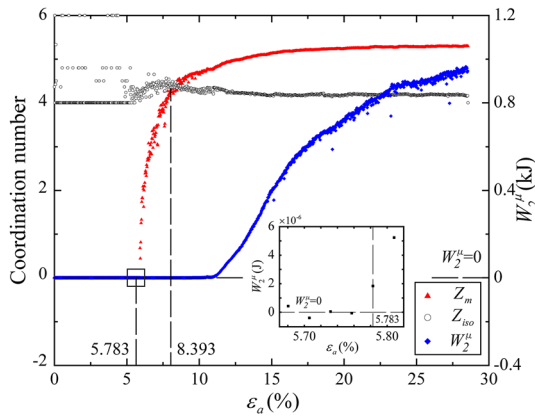


Fig. 17 Comparison between isostatic states identified from the isostatic coordination number-based criterion and from the second order work-based criterion for a frictional system subjected to constant volume monotonic shearing

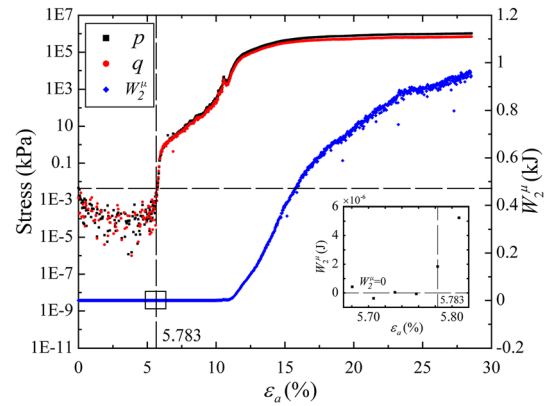


Fig. 18 Comparison between isostatic states identified from the second order work-based criterion and from the stress–strain curve for a frictional system subjected to constant volume monotonic shearing

Nonetheless, as can be seen in Fig. 18, the $W_2^\mu=0$ criterion indeed gives the same transition point at $\epsilon_a=5.783\%$. In this shear jamming scenario, the particulate system transforms from the unjammed state to the jammed state which means that the system has entered from the dynamic region to the quasi-static region. It is noteworthy that although the Eqs. 1 and 2 do not hold in the dynamic region, the $W_2^\mu=0$ criterion is still the most effective approach to determine the jamming (unjammed) transition compared with other methods.

5.4 Cyclic liquefaction of a frictional system (shear unjamming)

Shear could not only lead an unjammed system to jam, but may also make an initially jammed system become unjammed. Figure 19 shows the stress–strain curves of two frictional samples subjected to constant-volume cyclic triaxial shearing. The samples are initially in a jammed state with $\phi=0.6327$ sustaining the same amount of initial mean stress $p_{ini}=100$ kPa. They were subjected to cyclic sinusoidal loading with different amplitudes of q i.e., q_{cyc} . After a certain number of loading cycles following Eq. 3, both systems can no more maintain a stable state and flow like a liquid, which is characterized by abrupt drops of p to nearly zero and an

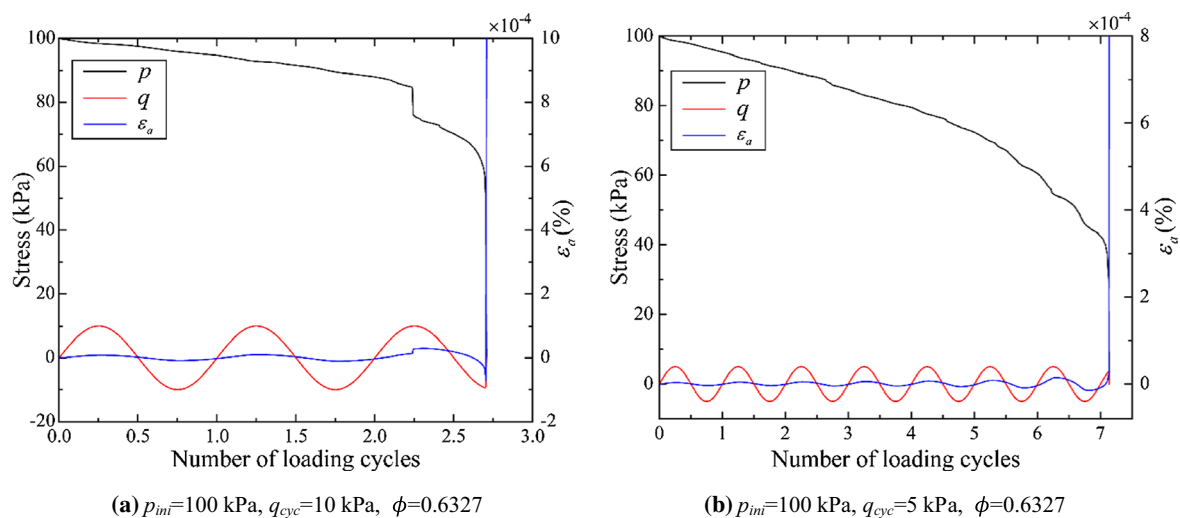


Fig. 19 Stress–strain curves of two frictional systems subjected to constant-volume cyclic loading

uncontrollable run-out axial deformation. As can be seen in Fig. 20, for both cases presented in Fig. 19, a clear jamming (unjamming) transition instant can also be identified for the $k=1.0$ force network. However, the data become much more scattered for the $k=2.2$ force network. In particular, it is difficult to derive an apparent jamming (unjamming) transition instant from $k=2.2$ force network for $q_{cyc}=10$ kPa simulations. Figure 21 shows the evolution of Z_m and Z_{iso} as well as the second order work during the cyclic loading process. Z_m decreases during loading and recovers during unloading, showing an overall decreasing trend. In contrast, Z_{iso} increases during loading and decreases during unloading with an overall increasing trend. The two intersect at around the 1.6705th and 6.1656th loading cycles for $q_{cyc}=10$ kPa and $q_{cyc}=5$ kPa cases, respectively. A higher q_{cyc} leads to a faster transition from jamming to unjamming. The second order work increases during loading and decreases during unloading, which suddenly drops below zero at around 2.71th and 7.135th loading cycles for the $q_{cyc}=10$ kPa and $q_{cyc}=5$ kPa cases, respectively, indicating that jamming (unjamming) transition occurs at these instants. Again, the jamming (unjamming) transition states identified by the two approaches coincide with each other.

5.5 Monotonic shearing on a frictional system (shear unjamming)

As stated in Sect. 3, the second order work-based criterion fails to identify the jamming (unjamming) transition point in some cases when failure happens progressively. Such an example is given below. Figure 22 gives the stress–strain curve during constant-volume static shearing of an initially jammed frictional system (GV). The mean effective stress

p decreases with the increase of axial strain but the deviatoric stress q increases at the initial state and then starts to decrease when the axial strain ϵ_a exceeds 1.718%, showing a typical static liquefaction phenomenon. As can be seen from Fig. 23, a clear jamming transition point can be identified based on the $k=1.0$ force network when ϵ_a reaches 0.4807% but no transition point can be obtained when the $k=2.2$ force network is considered. Clearly, the percolation analysis fails to capture the unjamming transition point. When the second order work-based criterion is applied in this example, the identified unjamming transition point is at $\epsilon_a=0.0285\%$ which is also different from that derived based on the stress–strain curve (Fig. 24). However, when the coordination number-based criterion is used, the identified unjamming transition point is consistent with that derived by the stress–strain curve (Fig. 25).

5.6 Discussion

Table 3 lists the jamming (unjamming) transition state identified based on different approaches for different loading scenarios. The $C^*=6$ criterion can be considered as a special case of the $Z_m=Z_{iso}$ criterion, where $Z_{iso}=6$. The well-recognized $Z_m=Z_{iso}$ criterion fails to predict the shear jamming instant. Similarly, the instant when the $k=1.0$ force network percolates in all three directions coincides with the jamming (unjamming) transition point at most scenarios except for the monotonic shear jamming and shear unjamming situation. As for energy-based approach, it can only predict the jamming (unjamming) transition state for the isotropic compression condition. Besides, although the second order work-based criterion succeeds in GI–GIV, it fails to

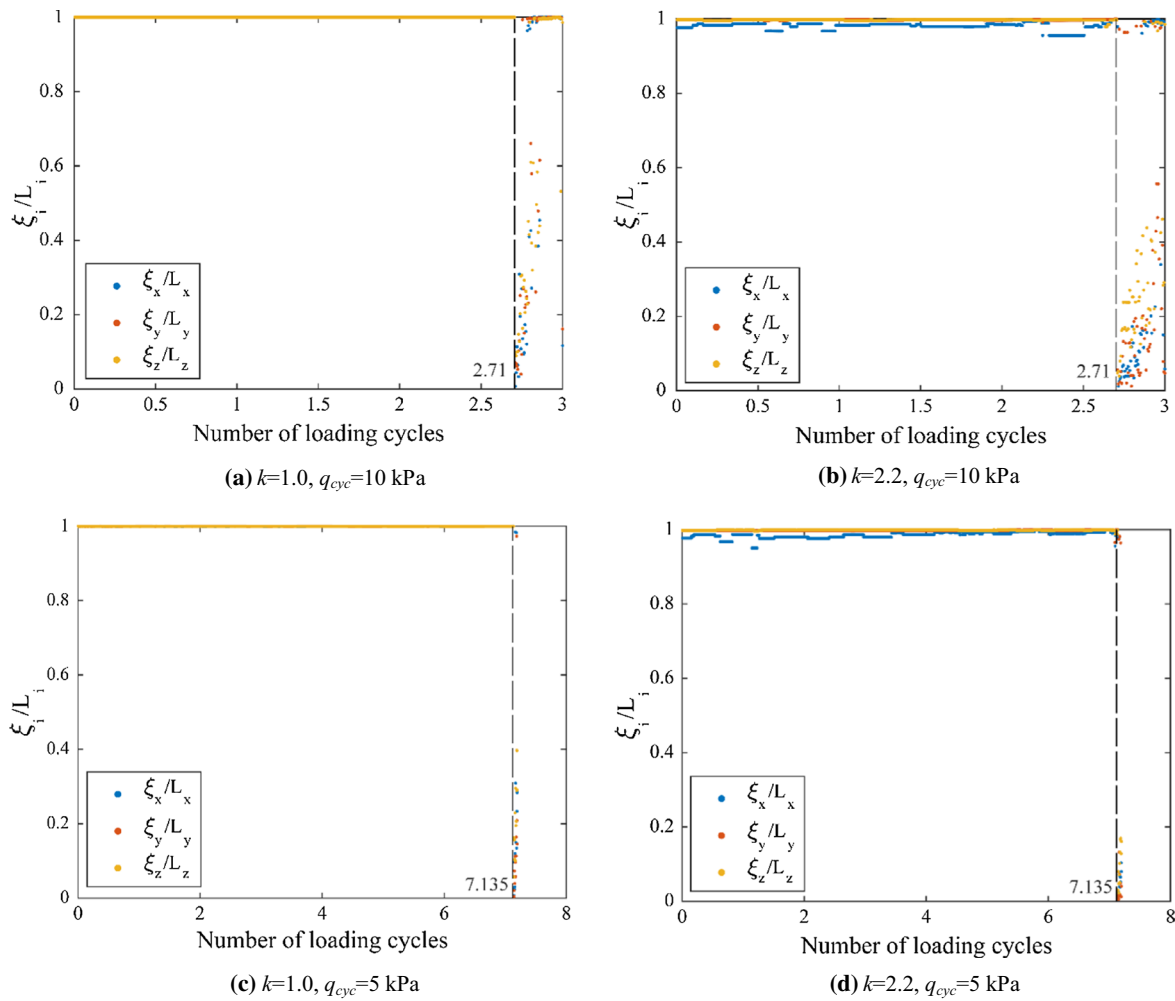


Fig. 20 Percolation analysis with different k values during constant volume cyclic loading of frictional systems ($p_{ini} = 100$ kPa, $\phi = 0.6327$)

predict the monotonic shear unjamming instant. Despite the progressive failure case (GV), the second order work-based criterion seems to be a more robust approach for identifying jamming (unjamming) transition, which yields results identical to that inferred from the nil stress condition.

6 Conclusion

This paper conducted a critical appraisal on the effectiveness of different approaches in identifying the jamming (unjamming) transition behavior of granular medium by performing DEM simulations on both frictionless and frictional systems subject to different types of loading protocols that represented isotropic jamming (unjamming) transition,

shear jammed and shear unjammed phenomena. A new second order work-based approach following Hill’s condition of initiation of instability was proposed as an alternative. The jamming (unjamming) transition states identified using different approaches were compared and the limitations of different approaches were discussed. It was found that the isostatic coordination number-based approach is applicable to various scenarios except for the shear jamming (unjamming) condition given that a correct isostatic coordination number can be derived. Similarly, when the $f \geq f_{avg}$ force network is examined the percolation analysis-based approach is effective for most loading protocols but fails to predict the correct jamming (unjamming) transition point for shear jamming and shear unjamming scenarios. Compared with the existing methods, the newly proposed second order

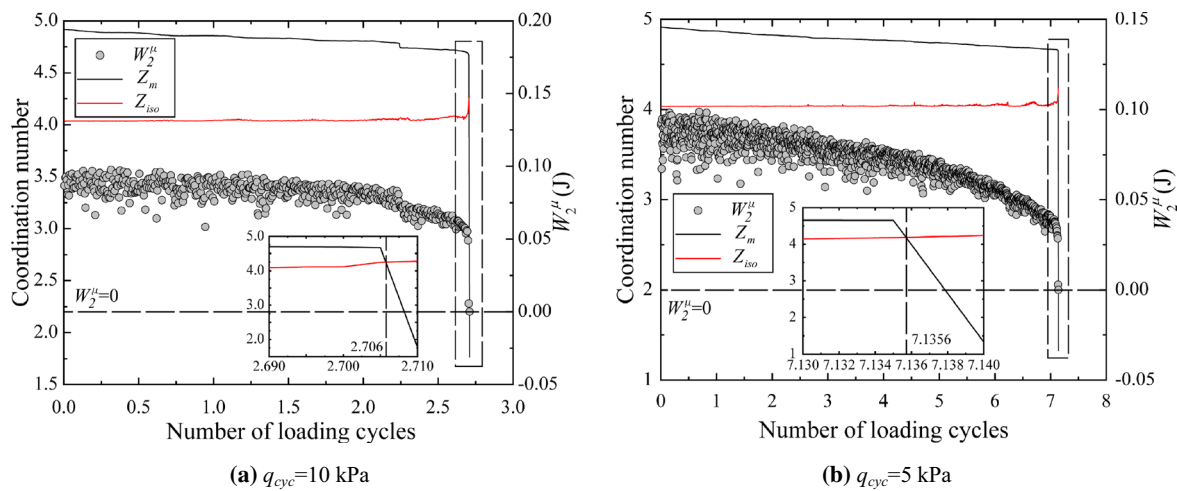


Fig. 21 Comparison between jamming (unjamming) transition states identified from the isostatic coordination number-based criterion and from the second order work-based criterion for frictional systems subjected to constant volume cyclic shearing ($p_{ini} = 100$ kPa, $\phi = 0.6327$)

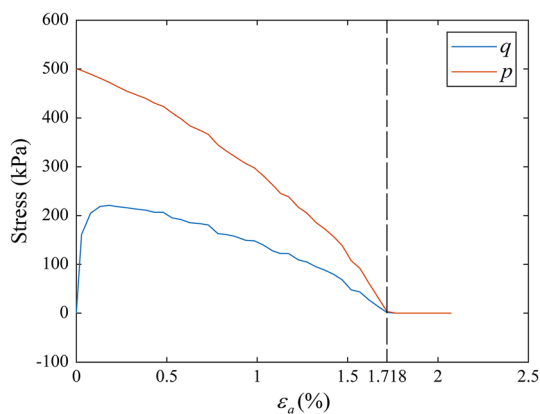


Fig. 22 Stress strain curves during constant volume monotonic shearing for a frictional system

It should also be noted that the instability underlined by the zero second-order work in soil mechanics is not always coincident with the unjamming state in physics. Nonetheless, the current study found that the Hill’s criterion did coincide with the jamming transition instants for isotropic compression, shear jamming and cyclic shear unjamming when liquefaction occurs instantaneously. However, it should be acknowledged that the Hill’s condition fails to interpret a correct jamming (unjamming) transition instant when there is a marginal duration for the granular materials to evolve from instability state to flow state. Notwithstanding, the Hill’s condition is more robust in comparison with existing approaches. It should also be acknowledged that in reality the stress paths of real materials may be more complex than the ones considered in this study. The applicability of the proposed approach needs to be further assessed in the future.

work-based approach is robust. Since it has been proved that the evolution trend of micro-scale and macro-scale second-order works are identical, the current study indicates that the second-order work approach is reliable when the micro-scale information is inaccessible. Therefore, it can be used to quantify the jamming diagram and analyze the jamming (unjamming) transition behavior of real materials other than the ideal photo-elastic materials.

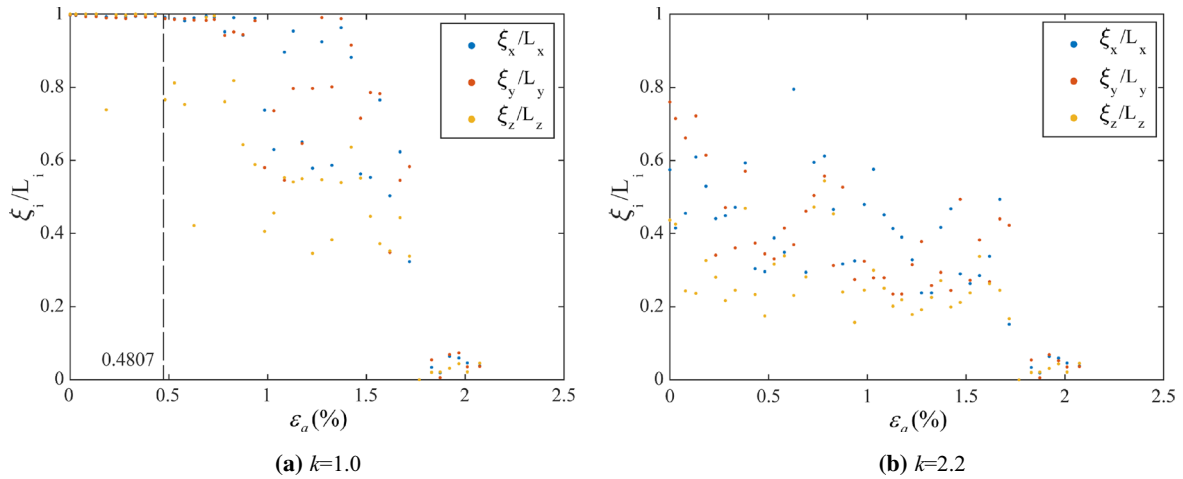


Fig. 23 Percolation analysis with different k values during constant volume monotonic shearing of a frictional system

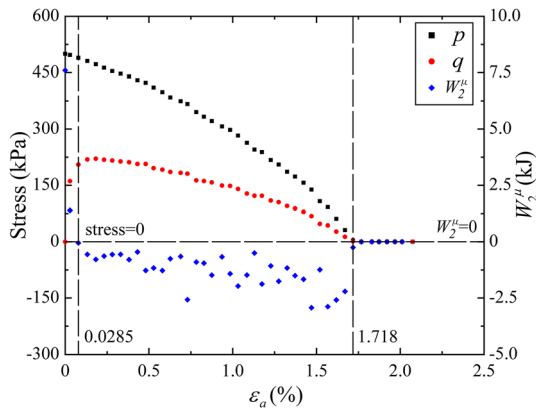


Fig. 24 Comparison between isostatic states identified from the second order work-based criterion and from the stress–strain curve for a frictional system subjected to constant volume monotonic shearing

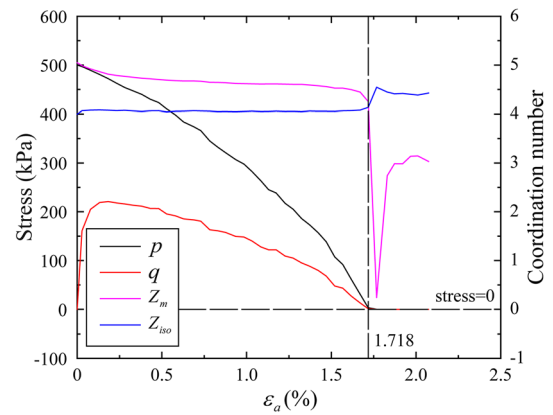


Fig. 25 Comparison between isostatic states identified from the coordination number-based criterion and from the stress–strain curve for a frictional system subjected to constant volume monotonic shearing

Table 3 Summary of jamming (unjamming) transition states identified based on different approaches

| ID | $C^r=6$ | $Z_m=Z_{iso}$ | $W_2^\mu=0$ | Percolation analysis $k=2.2$ | Percolation analysis suitable k | Energy-based approach | Stress–strain curve |
|-------------------------|---------|-----------------|-------------|------------------------------|--|-----------------------|---------------------|
| GI (ϕ) | 0.6531 | Same as $C^r=6$ | 0.6531 | 0.6531 | 0.6531 ($k=1.5$) 0.6531 ($k=1.0$) | 0.6531 | 0.6531 |
| GII (ϕ) | – | 0.6213 | 0.6213 | – | 0.6213 ($k=1.5$) 0.6213 ($k=1.0$) | 0.6223 | 0.6213 |
| GIII ($\epsilon, \%$) | – | 8.393 | 5.783 | 10.54 (fragile) | 8.495 ($k=1.5$) 7.932 ($k=1.0$) | – | 5.783 |
| GIV-1 (C_{num}) | – | 2.706 | 2.71 | – | 2.71 ($k=1.5$) 2.71 ($k=1.0$) | – | 2.71 |
| GIV-2 (C_{num}) | – | 7.135 | 7.135 | – | 7.135 ($k=1.5$) 7.136 ($k=1.0$) | – | 7.135 |
| GV ($\epsilon, \%$) | – | 1.718 | 0.0285 | – | 0.132 ($k=1.5$) 0.4807 ($k=1.0$) | – | 1.718 |

Acknowledgements The research was supported by the National Natural Science Foundation of China (Nos. 41877227 and 51509186).

Authors' contributions Mingze Xu: Analysis, figures and first draft writing; Zixin Zhang: research overseeing. Xin Huang: Conceptual and final editing.

Availability of data and material (data transparency) Available subject to request.

Code availability (software application or custom code) Not applicable.

Compliance with ethical standards

Conflict of interest The authors declare that they have no conflict of interest.

References

- Bi, D., Zhang, J., Chakraborty, B., Behringer, R.P.: Jamming by shear. *Nature* **480**, 355–358 (2011). <https://doi.org/10.1038/nature10667>
- Liu, A.J., Nagel, S.R.: Jamming is not just cool any more. *Nature* **396**(6706), 21–22 (1998). <https://doi.org/10.1038/23819>
- Ciamarra, M.P., Pastore, R., Nicodemi, M., Coniglio, A.: Jamming phase diagram for frictional particles. *Phys. Rev. E Stat. Nonlinear Soft Matter Phys.* (2011). <https://doi.org/10.1103/PhysRevE.84.041308>
- Göncü, F., Durán, O., Luding, S.: Jamming in frictionless packings of spheres: determination of the critical volume fraction. *AIP Conf. Proc.* **1145**, 531–534 (2009). <https://doi.org/10.1063/1.3179980>
- Van Hecke, M.: Jamming of soft particles: geometry, mechanics, scaling and isostaticity. *J. Phys. Condens. Matter* (2010). <https://doi.org/10.1088/0953-8984/22/3/033101>
- Wang, D., Ren, J., Dijksman, J.A., Zheng, H., Behringer, R.P.: Microscopic origins of shear jamming for 2D frictional grains. *Phys. Rev. Lett.* **120**, 208004 (2018). <https://doi.org/10.1103/PhysRevLett.120.208004>
- Huang, X., Hanley, K.J., Zhang, Z., Kwok, C.Y.: Structural degradation of sands during cyclic liquefaction: Insight from DEM simulations. *Comput. Geotech.* **114**, 103139 (2019). <https://doi.org/10.1016/j.compgeo.2019.103139>
- Shundyak, K., Van Hecke, M., Van Saarloos, W.: Force mobilization and generalized isostaticity in jammed packings of frictional grains. *Phys. Rev. E Stat. Nonlinear Soft Matter Phys.* **75**, 1–4 (2007). <https://doi.org/10.1103/PhysRevE.75.010301>
- Imole, O.I., Kumar, N., Magnanimo, V., Luding, S.: Hydrostatic and shear behavior of frictionless granular assemblies under different deformation conditions. *KONA Powder Part. J.* **30**, 84–108 (2012). <https://doi.org/10.14356/kona.2013011>
- Thornton, C.: Numerical simulations of deviatoric shear deformation of granular media. *Geotechnique* **50**, 43–53 (2000)
- Kumar, N., Luding, S.: Memory of jamming–multiscale models for soft and granular matter. *Granul. Matter* **18**, 1–21 (2016). <https://doi.org/10.1007/s10035-016-0624-2>
- Zhang, H.P., Makse, H.A.: Jamming transition in emulsions and granular materials. *Phys. Rev. E Stat. Nonlinear Soft Matter Phys.* **72**, 1–12 (2005). <https://doi.org/10.1103/PhysRevE.72.011301>
- Vinutha, H.A., Sastry, S.: Disentangling the role of structure and friction in shear jamming. *Nat. Phys.* **12**, 578–583 (2016). <https://doi.org/10.1038/nphys3658>
- Song, C., Wang, P., Makse, H.A.: A phase diagram for jammed matter. *Nature* **453**, 629–632 (2008). <https://doi.org/10.1038/nature06981>
- O'Hern, C.S., Langer, S.A., Liu, A.J., Nagel, S.R.: Force distributions near jamming and glass transitions. *Phys. Rev. Lett.* **86**, 111–114 (2001). <https://doi.org/10.1103/PhysRevLett.86.111>
- Xu, N., O'Hern, C.S.: Measurements of the yield stress in frictionless granular systems. *Phys. Rev. E Stat. Nonlinear Soft Matter Phys.* **73**, 1–7 (2006). <https://doi.org/10.1103/PhysRevE.73.061303>
- Rodney, D., Schuh, C.A.: Yield stress in metallic glasses: the jamming–unjamming transition studied through Monte Carlo simulations based on the activation–relaxation technique. *Phys. Rev. B Condens. Matter Mater. Phys.* (2009). <https://doi.org/10.1103/PhysRevB.80.184203>
- Urbani, P., Zamponi, F.: Shear yielding and shear jamming of dense hard sphere glasses. *Phys. Rev. Lett.* **118**, 1–5 (2017). <https://doi.org/10.1103/PhysRevLett.118.038001>
- Cunningham, N.: What is Yield Stress and why does it matter? (2016). <https://www.pcimag.com/ext/resources/WhitePapers/YieldStressWhitePaper.pdf>

20. Heussinger, C., Barrat, J.L.: Jamming transition as probed by quasistatic shear flow. *Phys. Rev. Lett.* **102**, 1–4 (2009). <https://doi.org/10.1103/PhysRevLett.102.218303>
21. Otsuki, M., Hayakawa, H.: Critical scaling near jamming transition for frictional granular particles. *Phys. Rev. E Stat. Nonlinear Soft Matter Phys.* **83**, 5–10 (2011). <https://doi.org/10.1103/PhysRevE.83.051301>
22. Göncü, F., Durán, O., Luding, S.: Constitutive relations for the isotropic deformation of frictionless packings of polydisperse spheres. *C. R. Méc.* **338**, 570–586 (2010). <https://doi.org/10.1016/j.crme.2010.10.004>
23. Luding, S.: About contact force-laws for cohesive frictional materials in 2d and 3d. In: Walzel, P., Linz, S., Krütle, C., Grochowski, R. (eds.) *Behavior of Granular Media*, Shaker Verlag, pp 137–147, band 9, Schriftenreihe Mechanische Verfahrenstechnik, ISBN 3-8322-5524-9 (2006)
24. Hidalgo, R.C., Grosse, C.U., Kun, F., Reinhardt, H.W., Herrmann, H.J.: Evolution of percolating force chains in compressed granular media. *Phys. Rev. Lett.* **89**, 1–5 (2002). <https://doi.org/10.1103/PhysRevLett.89.205501>
25. Smith, K.C., Fisher, T.S., Alam, M.: Isostaticity of constraints in amorphous jammed systems of soft frictionless Platonic solids. *Phys. Rev. E Stat. Nonlinear Soft Matter Phys.* **84**, 1 (2011). <https://doi.org/10.1103/PhysRevE.84.030301>
26. Geng, J., Behringer, R.P.: Slow drag in two-dimensional granular media. *Phys. Rev. E Stat. Nonlinear Soft Matter Phys.* **71**, 1–19 (2005). <https://doi.org/10.1103/PhysRevE.71.011302>
27. Olson Reichhardt, C.J., Reichhardt, C.: Fluctuations, jamming, and yielding for a driven probe particle in disordered disk assemblies. *Phys. Rev. E Stat. Nonlinear Soft Matter Phys.* **82**, 1–11 (2010). <https://doi.org/10.1103/PhysRevE.82.051306>
28. Candelier, R., Dauchot, O.: Journey of an intruder through the fluidization and jamming transitions of a dense granular media. *Phys. Rev. E Stat. Nonlinear Soft Matter Phys.* **81**, 1–12 (2010). <https://doi.org/10.1103/PhysRevE.81.011304>
29. Reichhardt, C., Reichhardt, C.J.O.: Aspects of jamming in two-dimensional athermal frictionless systems. *Soft Matter* **10**, 2932–2944 (2014). <https://doi.org/10.1039/c3sm53154f>
30. Lopera Perez, J.C., Kwok, C.Y., O’Sullivan, C., Huang, X., Hanley, K.J.: Exploring the micro-mechanics of triaxial instability in granular materials. *Geotechnique* **66**, 725–740 (2016). <https://doi.org/10.1680/jgeot.15.P.206>
31. Sawicki, A., Świdziński Waldemar, W.: Modelling the pre-failure instabilities of sand. *Comput. Geotech.* **37**, 781–788 (2010). <https://doi.org/10.1016/j.compgeo.2010.06.004>
32. Nicot F., Hadda N., Bourrier F., Sibille L., Tordesillas A., Darve F.: Micromechanical analysis of second order work in granular media. In: Chau K.T., Zhao J. (eds.) *Bifurcation and Degradation of Geomaterials in the New Millennium*. IWBDG 2014. Springer Series in Geomechanics and Geoengineering. Springer, Cham (2015). https://doi.org/10.1007/978-3-319-13506-9_11
33. Darve, F., Servant, G., Laouafa, F., Khoa, H.D.V.: Failure in geomaterials: continuous and discrete analyses. *Comput. Methods Appl. Mech. Eng.* **193**, 3057–3085 (2004). <https://doi.org/10.1016/j.cma.2003.11.011>
34. Nicot, F., Sibille, L., Darve, F.: Failure in rate-independent granular materials as a bifurcation toward a dynamic regime. *Int. J. Plast.* **29**, 136–154 (2012). <https://doi.org/10.1016/j.ijplas.2011.08.002>
35. Nicot, F., Daouadji, A., Laouafa, F., Darve, F.: Second-order work, kinetic energy and diffuse failure in granular materials. *Granul. Matter* **13**, 19–28 (2011). <https://doi.org/10.1007/s10035-010-0219-2>
36. Hadda, N., Nicot, F., Bourrier, F., Sibille, L., Radjai, F., Darve, F.: Micromechanical analysis of second order work in granular media. *Granul. Matter* **15**, 221–235 (2013). <https://doi.org/10.1007/s10035-013-0402-3>
37. Nicot, F., Darve, F.: A micro-mechanical investigation of bifurcation in granular materials. *Int. J. Solids Struct.* **44**, 6630–6652 (2007). <https://doi.org/10.1016/j.ijsolstr.2007.03.002>
38. Nova, R.: Controllability of the incremental response of soil specimens subjected to arbitrary loading programmes. *J. Mech. Behav. Mater.* **5**, 193–202 (1994)
39. Buscarnera, G., Dattola, G., Di Prisco, C.: Controllability, uniqueness and existence of the incremental response: a mathematical criterion for elastoplastic constitutive laws. *Int. J. Solids Struct.* **48**, 1867–1878 (2011). <https://doi.org/10.1016/j.ijsolstr.2011.02.016>
40. Yimsiri, S., Soga, K.: DEM analysis of soil fabric effects on behaviour of sand. *Géotechnique* **60**(6), 483–495 (2010). <https://doi.org/10.1680/geot.2010.60.6.483>
41. Huang, X., Hanley, K.J., Zhang, Z., Kwok, C., Xu, M.: Jamming analysis on the behaviours of liquefied sand and virgin sand subject to monotonic undrained shearing. *Comput. Geotech.* **111**, 1 (2019). <https://doi.org/10.1016/j.compgeo.2019.03.008>
42. Huang, X., Kwok, C.Y., Hanley, K.J., Zhang, Z.: DEM analysis of the onset of flow deformation of sands: linking monotonic and cyclic undrained behaviours. *Acta Geotech.* **13**, 1061–1074 (2018). <https://doi.org/10.1007/s11440-018-0664-3>
43. Liu, A.J., Nagel, S.R.: The Jamming Transition and the Marginally Jammed Solid. *Annu. Rev. Condens. Matter Phys.* **1**, 347–369 (2010). <https://doi.org/10.1146/annurev-conmatphys-070909-104045>

Publisher’s Note Springer Nature remains neutral with regard to jurisdictional claims in published maps and institutional affiliations.